

# Thermoelectric properties of flexible carbon nanotube and cotton textile nanocomposite-based cells

MUHAMMAD TARIQ SAEED CHANI<sup>1,\*</sup>, KHASAN S. KARIMOV<sup>2,3</sup>, KHALID AHMED AL ZAHRANI<sup>1,4</sup>, NAVED AZUM<sup>1</sup>, NOSHIN FATIMA<sup>5</sup>, HADI M. MARWANI<sup>1,4</sup>

<sup>1</sup>Center of Excellence for Advanced Materials Research, King Abdulaziz University, Jeddah 21589, P.O. Box 80203, Saudi Arabia

<sup>2</sup>Ghulam Ishaq Khan Institute of Engineering Sciences and Technology, Topi-23640, KPK, Pakistan

<sup>3</sup>Center for Innovative Development of Science and Technologies of Academy of Sciences, Rudaki Ave., 33, Dushanbe, 734025, Tajikistan

<sup>4</sup>Chemistry Department, Faculty of Science, King Abdulaziz University, Jeddah 21589, P.O. Box 80203, Saudi Arabia

<sup>5</sup>Faculty of Engineering, Technology and Built Environment, UCSI University, Kuala Lumpur, 56000, Malaysia

The design, fabrication and characterization of the carbon nanotubes (CNT)-cotton textile composite-based flexible thermoelectric cells are presented in this research. The piece of cotton textile was used as substrate and the constituent of CNT-cotton textile composite as well. To form the nanocomposite the CNTs were embedded in the cotton substrate by rubbing-in technique. The fabricated cells were investigated for temperature dependent Seebeck coefficient, thermoelectric resistance and short-circuit current. On rising temperature from 301 to 348 K the rise in the Seebeck coefficient and short-circuit current was found 2.15 times and 14 times, respectively, while the resistance of the cell fell by 1.53 time. Thermoelectric cells may be applied for the temperature gradient measurement and also as a converter (low power) of heat to electric energy. The major benefits of the fabricated thermoelectric cell are the following: use of environmentally friendly natural textile substrate, low-cost of materials (thermoelectric) and fabrication technology. The cell can be used as resistive temperature sensor because of its quasi-linear resistance–temperature relationship. This cell works as a multifunctional device. Textile substrates in the CNT-cotton textile composite-based thermoelectric cells make them shockproof.

(Received September 16, 2024; accepted February 3, 2025)

**Keywords:** Thermoelectric cell, Temperature gradient, Carbon nanotubes, Cotton textile, Flexible cell, Seebeck coefficient, Resistance, Short circuit current

## 1. Introduction

Thermoelectric energy harvesting from near to room temperature heat sources has attracted a significant interest. These sources of energy (heat) include consumer electronics, solar cells, home heating and wearable devices. For renewable power-generation applications several non-transparent materials with alluring thermoelectric characteristics were described [1-4], which involve tellurides, half-Heuslers, and silicides. Thermoelectric technology is becoming popular due to efficiency enhancement by using nanomaterials. The review of the thermoelectrics focusing on their present and potential applications was presented in ref. [5]. The flat-panel high-concentration solar TEGs (thermoelectric generators) with high performance were described in ref. [6]. Among the electronic devices, the fabrication technology of the thermoelectric cells is very simple. Regarding thermoelectric materials it is very well known that they are usually cheaper than solar cells' materials. But simultaneously thermoelectric devices ingest large quantities of materials as compared to solar cells. The carbon containing materials due to their environmentally friendly nature [7] seem desirable for the thermoelectric applications.

During the last years graphene was investigated for various thermoelectric properties [8-14]. The enormous

thermoelectric effect was observed in graphene by Dragoman et al. [8]. The augmentation of the figure of merit (thermoelectric) through the disorder in the armchair graphene-nanoribbons was studied by Ni et al. [14]. The enrichment of figure of merit (thermoelectric) in graphene-nanoribbons (edge-disordered) was also found by Sevincli et al. [13]. Moreover, in ref.[12] the oxygen-plasma treatment was used to enhance the thermopower of graphene films.

There are two disadvantages of using graphene in thermoelectric cells for energy conversion [11]. First, there is no band gap in graphene which causes a small Seebeck coefficient due to contrary influences of electrons and holes. Second, graphene has high thermal conduction due to which it possesses small  $ZT$ . Similarly, the reduction in lattice thermal-conductance and enhancement in the Seebeck coefficient of graphene can be achieved by nano-structuring and bandgap engineering. Therefore, the graphene may be possibly applied for the energy conversion [11].

Nano-structuring is one of the favorable techniques to design thermoelectric materials. Theoretically it was proven that heavy atoms and nanopores are helpful to make graphene nanoribbons attractive for thermoelectric applications [10]. The nanopores' two-dimensional array blocked the lattice thermal conduction in bulk. While at  $T \approx 40$  K the  $ZT$  increase to its highest ( $\approx 3$ ).

Composite of hetroatoms doped ethyl cellulose and MWCNT (multiwalled carbon nanotubes) were investigated for thermoelectric properties [16]. The ref. [17] presented the specified knowledge about the thermoelectric properties of CNTs. Kim et al. [18] prepared a composite of CNTs, PEDOT: PSS (poly (3,4-ethylenedioxythiophene) polystyrene sulfonate) and vinyl acetate ethylene (copolymer), that formed a segregated network. The thermal conductivity of the composite was diminished to  $0.3 \text{ W m}^{-1} \text{ K}^{-1}$  that may be regarded to the segregation by copolymer and also to various vibrational spectra and divergent bonding between CNTs and PEDOT: PSS. This network (of composite with 35 wt% SWCNTs) bridging of colloidal particles of PEDOT: PSS with CNT-CNT junctions guaranteed high electrical conductivity ( $400 \text{ S cm}^{-1}$ ). Chuizhou et al. [19] reported a PANI (polyaniline) coated network (freestanding) of individual CNTs and CNTs bundles, which were randomly entangled. The Seebeck coefficient of this CNTs-20 wt.% PANI composite was  $28 \mu\text{V K}^{-1}$ , while its electrical and thermal conductivities were up to  $60 \text{ S cm}^{-1}$  and  $\sim 0.5 \text{ W m}^{-1} \text{ K}^{-1}$ , correspondingly. Moreover, the ingredient (polymers & CNTs) mixing also improves the mechanical characteristics of the devices. A mechanically strong thermoelectric film (stretchable) fabricated by deposition of alternative layers of CNT-PAA (polyacrylic acid) and PEO (polyethylene oxide). On 30% stretching these films reserved thermoelectric performance up to 90% with crack-free surface [20]. The acquired thermoelectric and mechanical properties were regarded to the weak bonding and high chain mobility between PEO and PAA layers.

The CNTs-based temperature gradient sensors, CNTs-silicone adhesive composite-based thermoelectric cells, pristine $\alpha$ - $\text{Al}_2\text{O}_3$ co-dopedCdO-CNTs composite-based photo-thermoelectric cells and photo-thermo electrochemical flexible cells (Cu-orange dye aqueous solution/Cu) were designed, fabricated and investigated by our group [21-26]. Moreover, we also designed and constructed a solar thermoelectric generator, which was tested in the field conditions.

In persistence of our efforts to examine the thermoelectric properties of carbon containing materials, we are reporting here the thermoelectric properties of flexible CNT-cotton textile composite cells.

## 2. Experimental

For the fabrication of CNT-cotton textile composite-based cells the carbon nanotubes powder was purchased from Sun-Nanotech Co. Ltd., China. The natural cotton in the form of 0.6 mm thick sheet of cotton textile was bought

from the market. The cotton textile sheet was cut into pieces and used as substrate as well as one of the constituents of the Cotton-CNT composite. The composite was prepared using rubbing-in technique. This rubbing-in technology was described in detail by us in our previous works [27, 28]. Moreover, fabrication pressure was kept the same ( $65 \text{ g/cm}^2$ ) for all the samples. Fig. 1 shows the process flow diagram of the fabrication of CNT-cotton textile composite films-based flexible cells by rubbing-in technique.

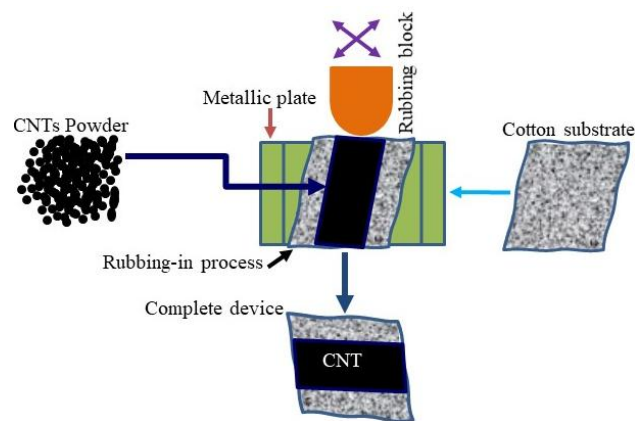


Fig. 1. Process flow diagram of the fabrication process of CNT-cotton textile composite films-based flexible thermoelectric cells (colour online)

The schematic diagrams of the fabricated CNT-cotton textile composite based thermoelectric cells are shown in Fig. 2a and 2b, while Fig. 2c and 2d show the pictures of the cotton substrate and the fabricated cells, respectively. The sizes of the textile substrates were  $3.5 \times 3.2 \text{ cm}^2$ . The length and the width of the CNT layer deposited on the cotton substrate by rubbing-in technology were equal to 30 mm 10 mm, correspondingly. The thickness of the CNT layer was equal to 10-12  $\mu\text{m}$ . Fig. 2a and 2b accordingly show the schematic diagrams of the front view and top view of the fabricated cells. The contact electrodes in Fig. 2b were used for the measurement of thermoelectric voltage. The thermocouples (Fig. 2b) were also used for the measurement of temperature gradient. To create the temperature and temperature gradient two petite sized heaters were used, which were thermally contacted to CNT films from two opposing sides across the length. In these thermoelectric cells the cotton textile played the double role: first of all, as composite with CNT, secondly, substrate for the cell. Fig. 2c shows the photograph of the cotton textile substrate with and without CNT film along with the scale.

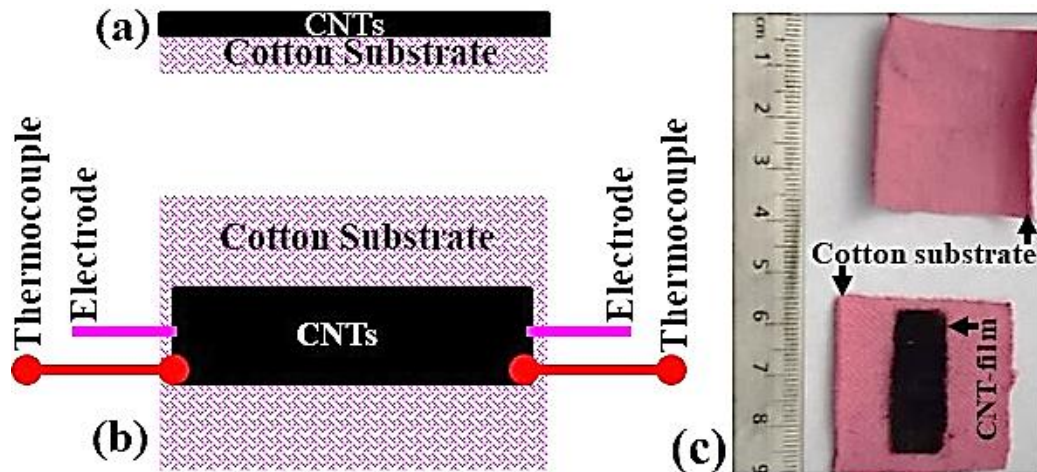


Fig. 2. The schematic illustration of the front view (a) and the top view (b) of the fabricated thermoelectric cells, and the photographs of the cotton substrate with and without CNT film (colour online)

For the X-ray diffraction (XRD) of CNT and cotton textile samples the Philips PW1830 XRD system was used. The structural information of both the materials was revealed by operating the system in  $\theta$ - $2\theta$  mode ( $15^\circ$  to  $80^\circ$ ) at room temperature using Cu-K $\alpha$  radiations at 40 kV (accelerating voltage) and 25 mA (tube current) with step size  $0.05^\circ$ . For each sample (natural textile and p-type CNTs) the scan was repeated three times to ensure the repeatability. The sample (natural textile and p-type CNTs) were scanned three times to confirm repeatability.

The DT 4253 digital multimeter was used for thermoelectric resistance, and voltage measurements. To create temperature gradient the resistive heaters were connected to the DC power supplies. The temperature

gradient was in the range of 6 to  $8^\circ\text{C}$  and was measured by thermocouples of the electronic device UT320D.

### 3. Results and discussions

The scanning electron micrograph of the CNTs-cotton textile nanocomposite is shown in Fig. 3. In the micrograph, the tube-like thin structure shows the CNTs in the composite, while the long-thick strands in the micrograph show the cotton fibers. The diameter of the cotton fibers is up to 200 nm and that of the CNTs is 30 to 50 nm.

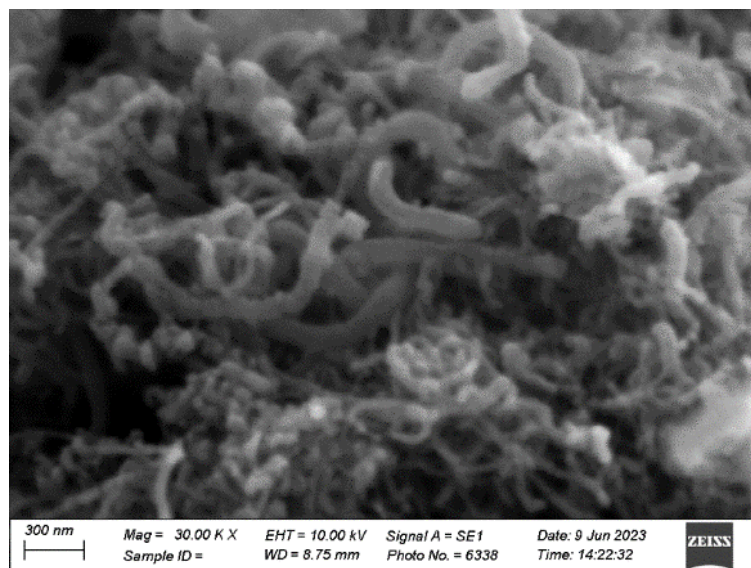


Fig. 3. The morphology of the CNTs-cotton textile composite

Fig. 4 shows the XRD scans of the textile (cotton) and CNTs powder. The XRD pattern of cotton cloth shows significantly high intensity diffraction peaks at  $2\theta$  of  $16.42^\circ$ ,  $23.17^\circ$ ,  $34.7^\circ$ , and  $38.28^\circ$ . The peaks at  $2\theta$  of  $16.42^\circ$  and  $23.17^\circ$  perfectly match with standard XRD database (PDF

00-050-2242) of ammonia cellulose and studies in literature [29]. The other peaks at  $2\theta$  of  $34.7^\circ$  and  $38.28^\circ$  perfectly match with standard XRD database (PDF 00-033-0289) of native cellulose [30].

The XRD scan of the CNTs powder shows major and broad peak around  $26.2^\circ$  (002) which is credited to the hexagonal graphite structure with significantly high conductivities (electrical). This peak shows the evenness with ICSD code: 031170. One additional peak observed at  $38.4^\circ$  may be the result of attached (to CNTs) functional group. The broad peak at  $2\theta$  angle  $44.3^\circ$  (101) is consistent with previous work [31].

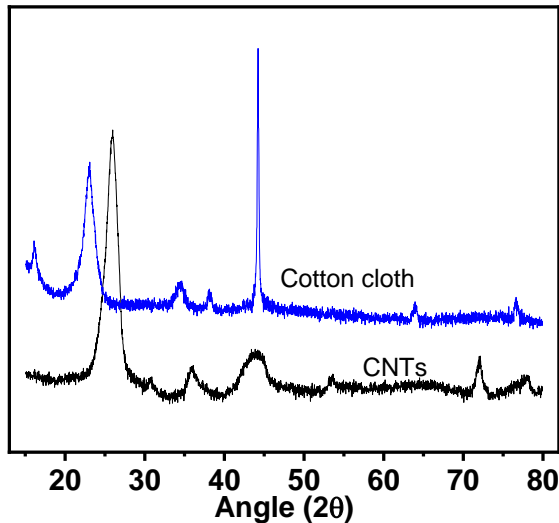


Fig. 4. XRD scans of the CNTs powder and the cotton textile (colour online)

Fig. 5 shows the thermoelectric voltage-temperature relationship of the CNT-cotton textile composite-based cell. On increasing temperature from 301 to 348 K the rise in the thermoelectric voltage was up to 2.6 times. The voltage rising behavior was quasi-linear. Usually, such type of relationships are very common in the conductive or extrinsic semiconducting materials [17, 32, 33].

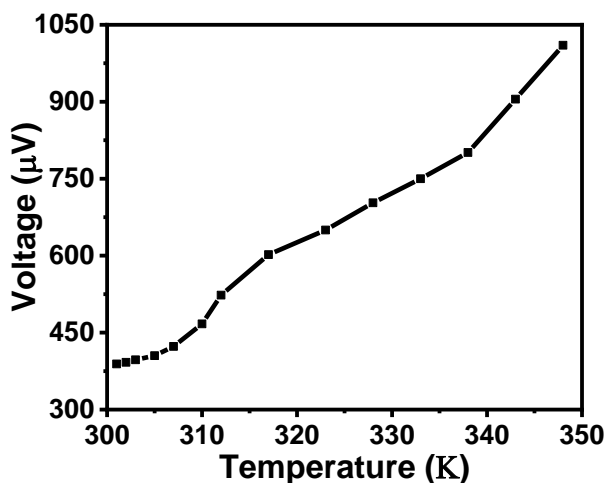


Fig. 5. The voltage (thermoelectric)-temperature behavior of CNT-cotton textile composite cells

The Seebeck or thermoelectric coefficient-temperature behavior of the fabricated CNT-cotton textile composite-based thermoelectric cells is shown in Fig. 6. The Eq.1 is

used to calculate the Seebeck coefficient [34]. Fig.6 shows that the value of coefficient (Seebeck/thermoelectric) is positive, which reveals that the fabricated samples are p-type semiconductor. The rise in temperature from 301 to 348 K results in the increase in the thermoelectric coefficient of the CNT-cotton textile composite-based cells up to 2.15 times.

$$\alpha = \frac{\Delta V}{\Delta T} \quad (1)$$

where,  $\Delta V$  and  $\Delta T$  are changes in voltage and temperature, while the  $\alpha$  represents the Seebeck coefficient.

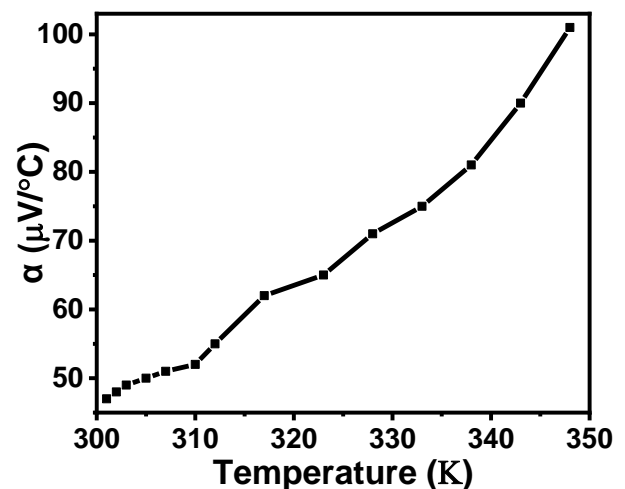


Fig. 6. The Seebeck coefficient-temperature behavior of the CNT-cotton textile composite-based cells

Fig. 7 shows the relationship of current (thermoelectric) and temperature of the fabricated CNT-cotton textile composite-based thermoelectric cells. As shown in the Fig.7, upon increasing temperature the thermoelectric current also increases. The rise in temperature from 301 to 348 K causes to increase thermoelectric current up to 14 times.

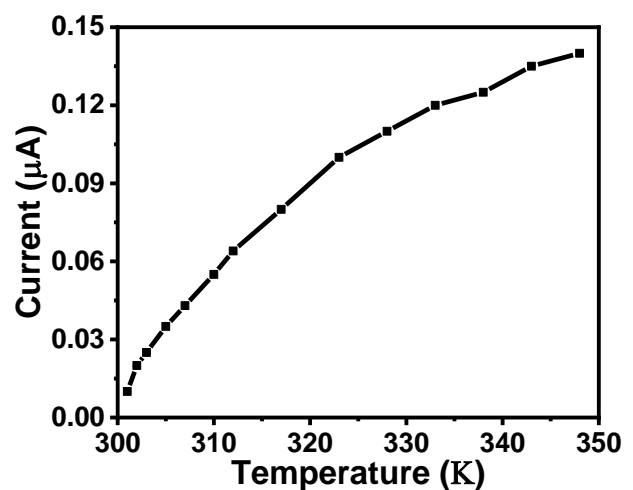


Fig. 7. The current (thermoelectric)-temperature relationship for the CNT-cotton textile composite-based cells

Fig. 8 shows the resistance-temperature relationship for the CNT-cotton textile composite-based cells. It shows that upon increasing temperature the resistance of the cell decreases. It indicates that the materials are showing semiconducting behavior. Moreover, upon changing temperature from 301 to 348 K the resistance of the fabricated cells was decreased by 1.5.

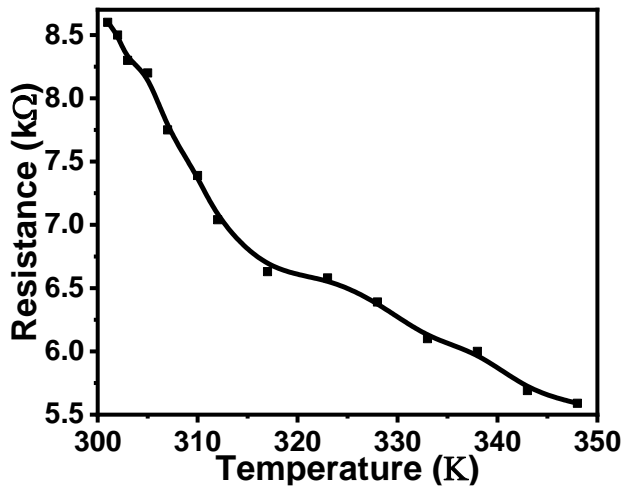


Fig. 8. Resistance-temperature relationship of CNT - cotton textile composite-based thermoelectric cell

The results of the fabricated cells may be discussed on two grounds. First, on the base of physical phenomena and second, on the base of the role of substrate (cotton textile) in the composite (CNT-cotton textile). As it is obvious that the carbon nanotubes depict the n/p-type or intrinsic materials' characteristics [17, 32]. Additionally, the CNTs may also behave like a material that have or not have energy bandgap [17, 33]. Moreover, the investigation of the fabricated thermoelectric cells shows that the used CNTs have the p-type material's characteristics. This argument is based on the results shown in Fig. 6, Fig.7 and Fig.8 that shows the effect of temperature on the Seebeck coefficient, current (thermoelectric) and resistance of the fabricated cells, respectively. As for as the role of cotton textile substrate in the electric characteristics of the fabricated cells is concerned; we are planning to comprehensively investigate it in near future. Basically, the composite of CNT-cotton textile may form charge-transfer complexes that is feasible also. Future research, particularly the investigation of the optical absorption of cotton textile, CNT and mixture of both can make clear this point as well.

To compare the fabricated CNT-cotton textile composite-based cells with the previously described devices on the base of technology, materials, Seebeck coefficient and operating temperature. The comparison presented in Table-1 illustrates that the fabricated cells are more attractive than the similar devices reported earlier.

Table 1. Comparison of the fabricated cells with the similar devices reported earlier

Sr. No	Technique	Material	Temperature (K)	Seebeck coefficient ( $\mu\text{V/K}$ )	Ref.
1	Pressing	MWCNT	300-440	15-20	[37]
2	Sheet	SWCNT	303-373	35-40	[38]
3	Free-standing film	CNT	303-373	48-54	[39]
4	Sponging	MWCNT	300-450	22-25	[40]
5	Compressing molding	MWCNT/EOC	-----	13.3	[41]
6	Rubbing-in	MWCNT- $\text{Ba}_2\text{Te}_3$ -Textile	301-351	88-105	[42]
7	lyophilization	CNT-PEDOT: PSS-Cotton aerogel	-----	43	[43]
8	SILAR	CuI/NC/Ct		90	[44]
9		MWCNT-EC	303-373	23-26	[16]
10	Rubbing-in	CNT-cotton textile	301-348	47-102	This study

MWCNT: Multiwalled carbon nanotubes, SWCNT: Single walled carbon nanotubes, EC: Ethyl cellulose, EOC: Ethylene-octene copolymer, SILAR: Successive Ionic Layer Adsorption and Reaction, CUI: copper iodide, NC: Nano cellulose, Ct: Commercial cotton.

The fabricated cells can be applied as elastic thermoelectric cells and modules that are used for low power applications. Moreover, these cells can also be used as temperature gradient measurement flexible thermoelectric sensor. The one of the significant achievements of this work is the exploitation of cotton textile as a substrate as well as the ingredient of the composite i.e., the composite of CNT and cotton textile. It may help to develop environmentally friendly and cost-effective power sources for the low power applications. The

efficiency of fabricated devices in terms of output voltage may be increased by adding any p-type thermoelectric material or thermoelectric conjugated polymers to the composite.

The simulation of various properties of the fabricated cells were also done using different mathematical functions. For the simulation of voltage-temperature, Seebeck coefficient-temperature and resistance-temperature relationships; following mathematical function was used with some modification:

$$f(x) = e^x \quad (2)$$

The revised form of the above mathematical function for the voltage-temperature relationships of the fabricated cells is the following:

$$V/V_0 = e^{k_1 \Delta T} \quad (3)$$

where  $V_0$  and  $V$  are the initial and instantaneous voltages of the fabricated cells, while the  $\Delta T$  is the change in temperature. The  $k_1$  is the voltage-temperature constant of cells and its value was calculated as  $2.03 \times 10^{-2}/K$ . The results of simulation are in good agreement with the obtained experimental results (as shown in Fig. 9a).

The revised form of the mathematical function shown in eq.2 for the relationship of Seebeck coefficient and temperature is the following:

$$\alpha/\alpha_0 = e^{k_2 \Delta T(0.2\Delta T + 0.8\Delta T_m)/\Delta T_m} \quad (4)$$

where the  $\alpha$  and  $\alpha_0$  are the instantaneous and initial Seebeck coefficient of the cell. The  $\Delta T_m$  is the maximum change in temperature and  $k_2$  is the Seebeck-temperature constant. The value of  $k_2$  was calculated as  $1.63 \times 10^{-2}/K$ . As shown in Fig.9b the simulated results are closely matched with the experimental results.

The simulation of the current-temperature relationships was done by the following revised form of the function (mathematical) given in eq. 2:

$$I/I_0 = e^{-k_3 \Delta T(\Delta T_m/(0.87\Delta T + 0.13\Delta T_m))} \quad (5)$$

where  $I_0$  is the initial current, and the  $I$  is the instantaneous current of the fabricated cell. The  $k_3$  is the current-temperature constant and was calculated as  $-5.62 \times 10^{-2}/K$ . The comparison of the results (simulated and experimental) is shown in Fig. 10a. These results are closely matched with each other.

The simulation of the resistance-temperature relationships was done by the following revised form of the function given in eq. 2:

$$R/R_0 = e^{k_4 \Delta T(\Delta T_m/(0.5\Delta T + 0.5\Delta T_m))} \quad (6)$$

where  $R_0$  is the initial resistance, and the  $R$  is the instantaneous resistance of the fabricated cell. The  $k_4$  is resistance-temperature constant and was calculated as  $-9.2 \times 10^{-3}/K$ . The experimental and the simulated results of resistance temperature relationships of the fabricated cells have been compared and shown in Fig. 10b. These simulated and experimental results (Fig. 10b) are in virtuous agreement with each other.

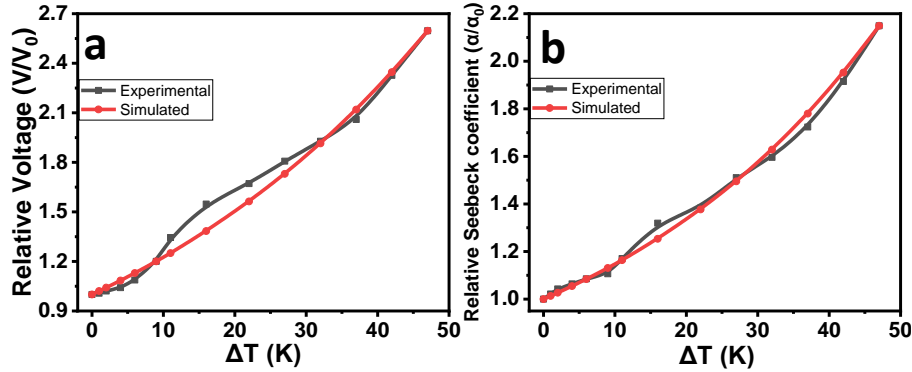


Fig. 9. Comparison of simulated and experimental results of thermoelectric voltage-temperature behavior (a) and Seebeck coefficient-temperature behavior (b) of CNT-cotton textile composite cells (colour online)

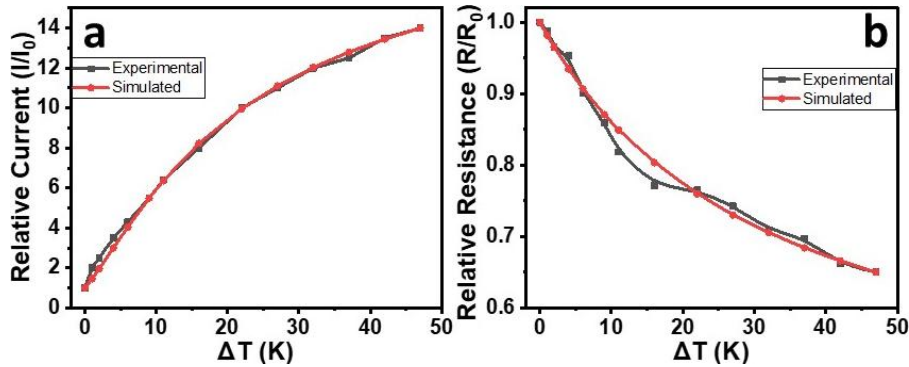


Fig. 10. Comparison of simulated and experimental results of thermoelectric current-temperature relationship (a) and resistant-temperature relationship (b) of CNT-cotton textile composite cells (colour online)

#### 4. Conclusion

This paper describes the fabrication and thermoelectric properties of semiconductive p-type carbon nanotubes and cotton textile composite-based thermoelectric cells fabricated by rubbing-in technology. The resistance-temperature, short-circuit current-temperature and thermoelectric coefficient-temperature characteristics depict that the CNT-cotton textile composite has similar characteristics as conventional p-type semiconductors. From practical point of view, it would be reasonable to add some conventional organic or/and inorganic thermoelectric materials to the CNT-cotton textile-based composite for the better performance of thermoelectric cells. As organic additives the polymers may have ability to increase the conductivity and Seebeck coefficient of the cells. Moreover, it can be expected that the electric properties of the optimal thermoelectric composite may be controlled by CNT, while, the mechanical properties, including flexibility may be controlled by conducting polymers. For this purpose, the different factors may be focused that include ingredient optimization, heat-treatment of the composite and the environmental effects of the composite. If there would be some negative effects, then to resolve these problems some ingredients or technology of fabrication may be changed. It should be taken into consideration that the CNT composite based thermoelectric cells are shockproof due to the use of cotton textile as a substrate. It may also be taken into account that the textile (cotton) affects the CNT because of the presence of pressure during rubbing-in process and also due to the formation of charge-transfer complexes between CNT and textile (due to electronic process). But this matter needs further investigations.

#### Acknowledgements

This project was funded by the Deanship of Scientific Research (DSR) at King Abdulaziz University, Jeddah, under grant no. (GPIP-1181-130-2024). The authors, therefore, acknowledge with thanks DSR for technical and financial support.

#### References

- [1] C. Yang, D. Souchay, M. Kneiß, M. Bogner, H. M. Wei, M. Lorenz, O. Oeckler, G. Benstetter, Y. Q. Fu, M. Grundmann, *Nature Communications* **8**, 16076 (2017).
- [2] Y. Gelbstein, *Acta Materialia* **61**, 1499 (2013).
- [3] K. Kirievsky, M. Shlimovich, D. Fuks, Y. Gelbstein, *Physical Chemistry Chemical Physics* **16**, 20023 (2014).
- [4] Y. Gelbstein, J. Tunbridge, R. Dixon, M. J. Reece, H. Ning, R. Gilchrist, R. Summers, I. Agote, M. A. Lagos, K. Simpson, *Journal of Electronic Materials* **43**, 1703 (2014).
- [5] S. B. Riffat, X. Ma, *Applied Thermal Engineering* **23**, 913 (2003).
- [6] D. Kraemer, B. Poudel, H.-P. Feng, J. C. Caylor, B. Yu, X. Yan, Y. Ma, X. Wang, D. Wang, A. Muto, K. McEnaney, M. Chiesa, Z. Ren, G. Chen, *Nature Materials* **10**, 532 (2011).
- [7] M. Sumino, K. Harada, M. Ikeda, S. Tanaka, K. Miyazaki, C. Adachi, *Applied Physics Letters* **99**, 188 (2011).
- [8] D. Dragoman, M. Dragoman, *Applied Physics Letters* **91**, 203116 (2007).
- [9] M. Zeng, W. Huang, G. Liang, *Nanoscale* **5**, 200 (2013).
- [10] P.-H. Chang, M. S. Bahramy, N. Nagaosa, B. K. Nikolic, *Nano Letters* **14**, 3779 (2014).
- [11] P. Dollfus, V. H. Nguyen, J. Saint-Martin, *Journal of Physics: Condensed Matter* **27**, 133204 (2015).
- [12] N. Xiao, X. Dong, L. Song, D. Liu, Y. Tay, S. Wu, L.-J. Li, Y. Zhao, T. Yu, H. Zhang, *ACS Nano* **5**, 2749 (2011).
- [13] H. Sevinçli, G. Cuniberti, *Physical Review B* **81**, 113401 (2010).
- [14] X. Ni, G. Liang, J.-S. Wang, B. Li, *Applied Physics Letters* **95**, 192114 (2009).
- [15] T. Ando, *NPG Asia Mater* **1**, 17 (2009).
- [16] B. Kumanek, G. Stando, P. S. Wróbel, M. Krzywiecki, D. Janas, *Synthetic Metals* **257**, 116190 (2019).
- [17] N. T. Hung, A. R. T. Nugraha, R. Saito, *Energies* **12**, 4561 (2019).
- [18] D. Kim, Y. Kim, K. Choi, J. C. Grunlan, C. Yu, *ACS Nano* **4**, 513 (2010).
- [19] C. Meng, C. Liu, S. Fan, *Advanced Materials* **22**, 535 (2010).
- [20] C. Cho, J. Son, *Nanomaterials* **10**(1),41 (2020).
- [21] M. T. S. Chani, K. S. Karimov, A. M. Asiri, N. Ahmed, M. M. Bashir, S. B. Khan, M. A. Rub, N. Azum, *PloS One* **9**, e95287 (2014).
- [22] M. T. S. Chani, S. B. Khan, A. M. Asiri, K. S. Karimov, M. A. Rub, *Journal of the Taiwan Institute of Chemical Engineers* **52**, 93 (2015).
- [23] T. Chani, K. Karimov, S. Khan, A. M. Asiri, *International Journal of Electrochemical Science* **10**, 5694 (2015).
- [24] M. T. S. Chani, A. M. Asiri, K. Karimov, M. M. Bashir, B. Khan, M. Rahman, *International Journal of Electrochemical Science* **10**, 3784 (2015).
- [25] M. T. S. Chani, A. Asiri, K. Karimov, J.-U. Nabi, A. Ahmed, I. Kiran, *J. Optoelectron. Adv. M.* **21**(9-10), 588 (2019).
- [26] M. T. S. Chani, K. S. Karimov, J.-U. Nabi, M. Hashim, I. Kiran, A. M. Asiri, *Int. J. Electrochem. Sci.* **13**, 11777 (2018).
- [27] M. T. S. Chani, A. M. Asiri, H. Karimov, *Google Patents*, 2021.
- [28] M. T. S. Chani, K. S. Karimov, H. M. Marwani, H. Muhammad, M. M. Zeeshan, A. M. Asiri, *International Journal of Electrochemical Science* **16**(7), 210712 (2021).

- [29] D. Parikh, D. Thibodeaux, B. Condon, *Textile Research Journal* **77**, 612 (2007).
- [30] K. Andress, *Zeitschrift für Physikalische Chemie* **136**, 279 (1928).
- [31] Y. Lu, X. Liu, W. Wang, J. Cheng, H. Yan, C. Tang, J.-K. Kim, Y. Luo, *Scientific Reports* **5**, 16584 (2015).
- [32] B. A. MacLeod, N. J. Stanton, I. E. Gould, D. Wesenberg, R. Ihly, Z. R. Owczarczyk, K. E. Hurst, C. S. Fewox, C. N. Folmar, K. H. Hughes, *Energy and Environmental Science* **10**, 2168 (2017).
- [33] L. Brownlie, J. Shapter, *Carbon* **126**, 257 (2018).
- [34] V. Derycke, R. Martel, J. Appenzeller, P. Avouris, *Applied Physics Letters* **80**, 2773 (2002).
- [35] S. K. P. G. C. Christakudis, E. S. Avilov, L. E. Shelimova, *Physica Status Solidi* **16**, 536 (1989).
- [36] D. Hayashi, Y. Nakai, H. Kyakuno, Y. Miyata, K. Yanagi, Y. Maniwa, *Applied Physics Express* **13**, 015001 (2019).
- [37] N. Salah, N. A. Alhebshi, Y. N. Salah, H. N. Alshareef, K. Koumoto, *Journal of Applied Physics* **128**, 235104 (2020).
- [38] W. Huang, E. Tokunaga, Y. Nakashima, T. Fujigaya, *Science and Technology of Advanced Materials* **20**(1), 97 (2019).
- [39] B. Kumanek, G. Stando, P. Stando, K. Matuszek, K. Z. Milowska, M. Krzywiecki, M. Gryglas-Borysiewicz, Z. Ogorzałek, M. C. Payne, D. MacFarlane, D. Janas, *Scientific Reports* **11**, 8649 (2021).
- [40] X. Yang, J. Cui, K. Xue, Y. Fu, H. Li, H. Yang, *Nanotechnology Reviews* **10**, 178 (2021).
- [41] P. Slobodian, P. Riha, R. Olejnik, M. Kovar, P. Svoboda, *Journal of Nanomaterials* **2013**, 792875 (2013).
- [42] M. T. S. Chani, K. S. Karimov, U. Asghar, R. Ali, A. M. Asiri, *Journal of Materials Science: Materials in Electronics* **34**, 1976 (2023).
- [43] He, M. Liu, J. Cai, Z. Li, Z. Teng, Y. Hao, Y. Cui, J. Yu, L. Wang, X. Qin, *Engineering* **39**, 235 (2024).
- [44] N. P. Klochko, V. A. Barbash, K. S. Klepikova, S. I. Petrushenko, V. R. Kopach, O. V. Yashchenko, S. V. Dukarov, V. M. Sukhov, A. L. Khrypunova, *J. Mater. Sci.: Mater. Electron.* **33**, 16466 (2022).

---

\*Corresponding author: tariqchani1@gmail.com